Article

Iron Blast Furnace Slag/Hydrated Lime Sorbents for Flue Gas Desulfurization

Chiung-Fang Liu, and Shin-Min Shih

Environ. Sci. Technol., **2004**, 38 (16), 4451-4456 • DOI: 10.1021/es030347c

Environ. Sci. Technol. **2004**, *38,* 4451−4456

Iron Blast Furnace Slag/Hydrated Lime Sorbents for Flue Gas Desulfurization

CHIUNG-FANG LIU AND SHIN-MIN SHIH*

Department of Chemical Engineering, National Taiwan University, Taipei, Taiwan 106

Sorbents prepared from iron blast furnace slag (BFS) and hydrated lime (HL) through the hydration process have been studied with the aim to evaluate their reactivities toward SO_2 under the conditions prevailing in dry or semidry flue gas desulfurization processes. The BFS/HL sorbents, having large surface areas and pore volumes due to the formation of products of hydration, were highly reactive toward SO_2, as compared with hydrated lime alone (0.24 in Ca utilization). The sorbent reactivity increased as the slurrying temperature and time increased and as the particle size of BFS decreased; the effects of the liquid/solid ratio and the sorbent drying conditions were negligible. The structural properties and the reactivity of sorbent were markedly affected by the BFS/HL ratio; the sorbent with 30/70 ratio had the highest 1 h utilization of Ca, 0.70, and SO_2 capture, 0.45 g SO_2/g sorbent. The reactivity of a sorbent was related to its initial specific surface area (S_{g0}) and molar content of Ca (M^{-1}); the 1 h utilization of Ca increased almost linearly with increasing S_{g0}/M. The results of this study are useful to the preparation of BFS/HL sorbents with high reactivity for use in the dry and semidry processes to remove SO_2 from the flue gas.

Introduction

Reducing SO_2 emissions from power plants is a major issue for environmental protection. Many flue gas desulfurization (FGD) processes are available for the reduction of SO_2 emission (*1*−*3*). The dry and semidry FGD processes have the advantages of lower capital cost and easier waste treatment in comparison with the wet processes commonly adopted in power plants; however, the utilization of the sorbent, which is mostly hydrated lime (HL), in the former processes is low. The economics of these processes can be greatly improved by increasing the sorbent reactivity and utilization.

Many researchers found that sorbents prepared from HL and silica-containing materials, such as fly ash (*4*−*22*), diatomaceous earths (*23*−*24*), quartz (*25*−*26*), silica fume (*27*−*31*), and iron blast furnace slag (*32*), are more reactive toward SO_2 than HL. The silica-enhanced lime sorbents were prepared through a hydration process in which silica reacts with HL to form foil-like calcium silicate hydrates in the presence of water; this reaction is called "pozzolanic reaction" (*33*). It has been confirmed that the pozzolanic reaction, which results in sorbents with large surface areas, is responsible for the enhancement of sorbent reactivity (*4*, *9*, *10*, *13*, *22*).

* Corresponding author phone: 886-2-23633974; fax: 886-2-23623040; e-mail: smshih@ntu.edu.tw.

Among the silica-containing materials, fly ash has attracted the most attention so far. Iron blast furnace slag (BFS), mainly composed of CaO, SiO_2, and Al_2O_3, is similar in constituents to fly ash, but its CaO content is higher. The literature on sorbents prepared from BFS, however, is scarce (*32*). Only recently, Brodnax and Rochelle (*32*) reported that sorbents prepared from HL and BFS indeed had greater surface areas and higher reactivities than HL. Successful use of sorbents prepared from BFS reduces not only the operating cost of a desulfurization process but also the amount of waste BFS. Thus, this subject deserves further study.

In this work, sorbents were prepared from BFS and HL under different preparation conditions. The sorbents were characterized and subjected to reaction with SO_2, with the aim to elucidate the effects of the preparation conditions on their structural properties and hence their reactivities toward SO_2.

Experimental Procedure

Preparation of Sorbents. The HL used in this study was reagent grade $Ca(OH)_2$ (Hayashi Pure Chemical Industries, Ltd). The BFS was supplied by the China Hi-Ment Corporation in two size ranges, high fineness (HBFS) and general fineness (GBFS). The physical properties and chemical compositions of the HL and BFS are listed in Table 1.

The hydration of BFS and HL using deioned water was performed in a 250 mL polypropylene conical flask, keeping constant the total solid weight at 8 g. The BFS/HL weight ratios tested were 0/100, 10/90, 30/70, 50/50, 70/30, 90/10, and 100/0. The water/solid (L/S) weight ratios tested were 5/1, 10/1, 15/1, and 20/1. After pouring the solids and water into the flask, it was sealed with a rubber stopper at the mouth and inserted into a thermostat. The slurry was stirred with a magnetic stirrer for a certain period of time, 0.42−32 h. The slurrying temperatures used were 25−95 °C.

The slurry was typically vacuum-dried at 105 °C for 8 h. To study the effect of drying conditions on sorbent reactivity, some slurry samples prepared with a HBFS/HL ratio of 30/70, L/S ratio of 10/1, 65 °C, and 16 h slurrying time were dried under different conditions: vacuum and 105 °C for 2 h, vacuum and 35 °C for 24 h, and ambient pressure and 105 °C for 8−168 h. The dry cake was crushed into powder and sealed in a bottle before use.

Sulfation Test. The sulfation test was performed by reacting a sample of about 30 mg with a gas mixture containing N_2, H_2O, and 1000 ppm SO_2 in a differential fixed-bed reactor at 60 °C and 70% relative humidity (RH). The conditions was selected so as to simulate the typical conditions in the bag filters of a spray-drying FGD process. CO_2 and O_2 were not added to make the synthetic flue gas because the test was only conducted for screening purposes. Our preliminary tests, however, showed that the presence of CO_2 and O_2 had negligible effect on the sulfation of sorbents. The sample was dispersed into the quartz wool inserted in the sample pan; the pan was perforated at the bottom to facilitate the passage of the gas. The experimental setup and procedure were similar to those used by Ho and Shih (*10*).

The utilization of Ca (X) for a reacted sample was defined as the SO_3^{2-}/Ca^{2+} molar ratio. The SO_3^{2-} content in a reacted sample was determined by iodometric titration and the Ca^{2+} content by EDTA titration. The details of these analyses were described by Ho and Shih (*11*).

The SO_2 capture (SC) for a reacted sample was defined as the ratio of the weight of the SO_2 captured to the initial

10.1021/es030347c CCC: $27.50
Published on Web 07/17/2004

TABLE 1. Physical Properties and Compositions of Hydrated Lime and Iron Blast Furnace Slag

material	d_P (μm)	density (g/cm^3)	S_{g0} (m^2/g)	composition (wt %)									
				$Ca(OH)_2$	CaO	SiO_2	Al_2O_3	MgO	Fe_2O_3	SO_3	alkalinity	S	ignition loss
$Ca(OH)_2$	6.0	2.30	10.0	>95									
HBFS	5.9	2.90	1.5		42.00	33.47	13.78	6.98	0.39	0.42	1.67	0.27	1.67
GBFS	7.9	2.89	1.4		42.32	34.29	14.52	6.77	0.18	0.44	1.83	0.23	0.64

TABLE 2. Preparation Conditions (L/S = 10/1), Structural Properties, and Sulfation Results for BFS/HL Sorbents[c]

BFS/HL weight ratio	slurrying temp (°C)	slurrying time (h)	L/S	M (g sorbent/ mol Ca)	d_P (μm)	S_{g0} (m^2/g)	V_m (2−50 nm) (cm^3/g)	V_t (2−300 nm) (cm^3/g)	X[b]	SC (g SO_2/ g sorbent)
raw HBFS			10/1	146	5.9	1.5	0.005	0.008	0.03(3)	0.01
HBFS/HL										
100/0	65	16	10/1	147	20.8	17.1	0.130	0.135	0.11(4)	0.05
90/10	65	16	10/1	139	17.2	25.9	0.192	0.197	0.43(3)	0.20
70/30	65	16	10/1	128	14.1	31.1	0.224	0.229	0.51(4)	0.26
50/50	65	16	10/1	114	12.2	32.6	0.243	0.252	0.60(3)	0.34
30/70	65	16	10/1	96	7.2	28.9	0.205	0.212	0.70(3)	0.46
10/90	65	16	10/1	82	7.0	23.6	0.137	0.141	0.45(2)	0.35
0/100	65	16	10/1	75	5.8	11.8	0.073	0.077	0.24(3)	0.20
30/70	25	16	10/1	97	7.2	22.3	0.167	0.174	0.39(3)	0.25
30/70	35	16	10/1	99					0.57(3)	0.37
30/70	45	16	10/1	98	7.4	28.8	0.185	0.192	0.58(3)	0.38
30/70	55	16	10/1	98					0.64(2)	0.42
30/70	75	16	10/1	97					0.67(3)	0.44
30/70	85	16	10/1	99	7.2	31.1	0.204	0.206	0.69(3)	0.45
30/70	95	16	10/1	97					0.68(2)	0.45
30/70	65	0.42	10/1	100	7.1	26.8	0.188	0.194	0.60(3)	0.38
30/70	65	1	10/1	97					0.59(3)	0.39
30/70	65	2	10/1	101					0.63(3)	0.40
30/70	65	4	10/1	98	7.2	28.4	0.191	0.197	0.62(3)	0.40
30/70	65	8	10/1	100					0.67(2)	0.43
30/70	65	32	10/1	99	7.3	30.9	0.194	0.201	0.72(3)	0.47
30/70	65	16	5/1	101					0.60(3)	0.38
30/70	65	16	15/1	100					0.69(2)	0.44
30/70	65	16	20/1	100					0.70(2)	0.45
raw GBFS			10/1	149	7.9	1.4	0.005	0.007	0.02(3)	0.01
GBFS/HL										
100/0[a]	65	16	10/1	151	23.8	12.4	0.076	0.079	0.08(3)	0.03
90/10[a]	65	16	10/1	145	17.5	28.1	0.203	0.209	0.35(4)	0.15
70/30[a]	65	16	10/1	128	15.2				0.42(4)	0.21
50/50[a]	65	16	10/1	114	13.7	32.8	0.195	0.200	0.52(3)	0.29
30/70[a]	65	16	10/1	97	9.7	26.0	0.151	0.154	0.61(3)	0.40
10/90[a]	65	16	10/1	83	7.2				0.36(3)	0.28

[a] GBFS. [b] No. of sulfation runs. [c] Sulfation conditions: 60 °C, 70% RH, and 1000 ppm SO_2 for 1 h.

weight of the sample. SC is related to the utilization of Ca by

$$SC = M_{SO2} \cdot M^{-1} \cdot X \quad (1)$$

where M_{SO2} is the molecular weight of SO_2 and M is the initial sample weight per mole of Ca. M was determined from the Ca^{2+} content of an unreacted sample, which was measured by EDTA titration. The values of M of the sorbents are summarized in Table 2.

Chemical and Physical Analyses. The samples were subjected to X-ray diffraction (XRD) analysis using a Mac Science M03XHF X-ray diffractometer with Cu target. Scanning electron microscope (SEM), Hitachi S-2400, was used to observe the morphology of a sample. The sorbent particle size was measured by laser diffraction using a Coulter LS-230 analyzer. The specific surface area of sorbent was determined from the nitrogen adsorption data by the BET method, and the pore volume distribution was determined from the nitrogen desorption isotherm by the BJH method, using a Micromeritics ASAP 2010 analyzer.

Results and Discussion

XRD Analysis. The XRD patterns of some sorbents prepared at different conditions are shown in Figure 1. The pattern of the treated BFS (100/0), which is similar to that of the raw BFS, has a mild hump in the range of 2θ from 20° to 40° with a peak at about 30°, characterizing the amorphous portion of the slag. The pattern indicates that the crystalline portion of the slag is very small. The peak at 2θ of 29.6° indicates the presence of a small amount of $CaCO_3$ in the slag. The peak of $CaCO_3$ did not appear for freshly prepared samples.

For BFS/HL (90/10−10/90) sorbents, the patterns showed the characteristic peaks of $Ca(OH)_2$ and the hydration products, calcium silicate hydrates (e.g., ill-crystallized tobermorites (*33*), 2θ = 29°−29.8°, 32°, and 49.8°), calcium aluminum oxide hydrate ($Ca_3Al_2O_6 \cdot xH_2O$, 2θ = 11.56°, 23.58°, 31.25°, 35.56°), and calcium aluminum silicate hydroxide ($Ca_3Al_2(SiO_4)(OH)_8$, 2θ = 28.88°, 32.37°, 39.91°, 45.21°). The peaks of hydration products, such as calcium silicate hydrates, are weak; thus, it is difficult to identify all of them contained in a sorbent. Also, it is difficult to tell how the sorbent preparation conditions affected their formations. Nevertheless, their peaks seemed to be stronger for sorbents prepared

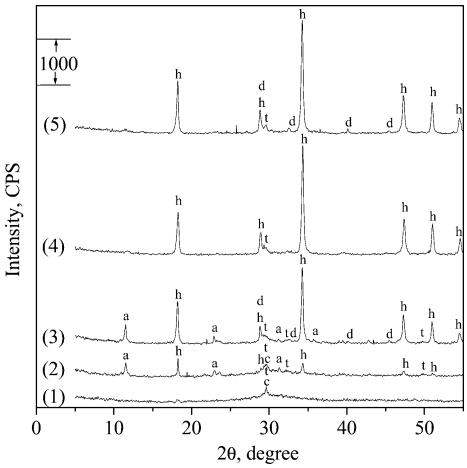

FIGURE 1. XRD patterns of HBFS/HL sorbents prepared at various slurrying conditions: (1) 100/0 wt ratio, 65 °C, L/S = 10/1, and 16 h, (2) 90/10 wt ratio, 65 °C, L/S = 10/1, and 16 h, (3) 30/70 wt ratio, 65 °C, L/S = 10/1, and 16 h, (4) 30/70 wt ratio, 65 °C, L/S = 10/1, and 0.42 h, and (5) 30/70 wt ratio, 25 °C, L/S = 10/1, and 16 h. (a: $Ca_3Al_2O_6 \cdot xH_2O$, c: calcite, d: $Ca_3Al_2(SiO_4)(OH)_8$, h: $Ca(OH)_2$, t: calcium silicate hydrates).

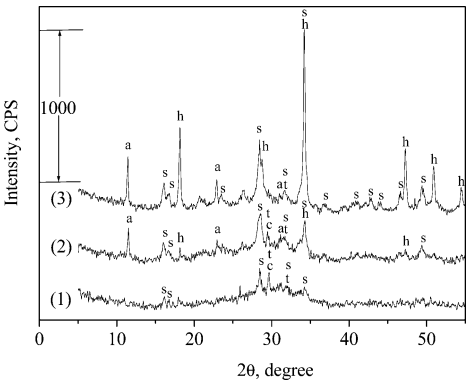

FIGURE 2. XRD patterns of sulfated HBFS/HL sorbents prepared with various weight ratios: (1) 100/0, (2) 90/10, and (3) 30/70. Slurrying conditions: 65 °C, L/S = 10/1, and 16 h; sulfation conditions: 60 °C, 70% RH, 1000 ppm SO_2, and 1 h. (a: $Ca_3Al_2O_6 \cdot xH_2O$, c: calcite, h: $Ca(OH)_2$, s: $CaSO_3 \cdot 0.5H_2O$, t: calcium silicate hydrates).

with a BFS/HL ratio of 30/70, or with a longer slurrying time, or with a higher slurrying temperature (Figure 1), and unaffected by the L/S ratio.

Figure 2, the patterns of some sorbents which had reacted with SO_2, shows that the reaction product is $CaSO_3 \cdot 0.5H_2O$ and that the peaks of $Ca(OH)_2$ and hydration products become weaker as compared with those for the unreacted samples (Figure 1).

SEM Observation. The particles of the raw BFS are irregular in shape and have sharp edges and smooth surfaces, as shown in Figure 3a. As BFS alone was slurried and dried, the particles are covered with foil-like substances and fine particles, as seen from Figure 3b, indicating that BFS itself can react with water to form appreciable amounts of hydration products.

Figure 3c shows the typical BFS/HL sorbent particles. The particles compose of foil-like substances and have a highly porous structure. As shown in Figure 3d, the particles of sulfated samples appear almost the same as the unreacted particles (Figure 3c), but the foil-like substances seem to be thicker.

Particle Size, Specific Surface Area, and Pore Volume Measurements. The volume mean particle diameters (d_P), specific surface areas (S_{g0}), and specific pore volumes (V_m and V_t) of sorbents are summarized in Table 2.

The mean particle diameters of HBFS/HL sorbents, 7−21 μm, are slightly smaller than those of GBFS/HL sorbents at each BFS/HL ratio for ratios ≥ 10/90. The mean particle diameter increases with increasing BFS/HL ratio, being the largest at a ratio of 100/0. The mean particle diameter of the slurried $Ca(OH)_2$ is slightly smaller than that of the raw $Ca(OH)_2$, indicating that finer crystals were formed when $Ca(OH)_2$ recrystallized from the solution. The sorbents with ratios >10/90 have mean particle diameters larger than that of the raw BFS or $Ca(OH)_2$; this result reveals that the hydration products had caused the coherence of sorbent particles. The effects of slurrying temperature and time on the mean particle diameter of sorbent are negligible.

As seen in Tables 1 and 2, the specific surface areas of the raw $Ca(OH)_2$, HBFS, and GBFS are 10.0, 1.5, and 1.4 m^2/g, respectively, and they are much smaller than those of the BFS/HL sorbents. This comparison indicates the formation of substances of large surface area in the BFS/HL sorbents. The specific surface area of sorbent varies with the BFS/HL ratio and reaches a maximum at the ratio of 50/50; the maximum surface areas are 32.6 and 32.8 m^2/g for HBFS/HL and GBFS/HL sorbents, respectively. In addition, the specific surface area increases with increasing slurrying temperature and slurrying time; however, the effects of these two variables are not pronounced when the temperature was higher than 45 °C and the time longer than 0.42 h. Brodnax and Rochelle (*32*) reported similar effects of BFS/HL ratio and slurrying time on the specific surface area of sorbent, but the surface areas of their sorbents were larger, about 25−54 m^2/g for sorbents prepared with different BFS/HL ratios and 20 h slurrying time. This difference may be resulted from that the surface areas of their raw $Ca(OH)_2$ (21.6 m^2/g) and slag (3.6 m^2/g) were larger than those of ours and that their slurrying temperature (92 °C) was higher than those used in this study.

The nitrogen adsorption and desorption isotherms for the BFS/HL sorbents and the starting BFS and $Ca(OH)_2$ indicated that they were materials with porosity in the mesopore range and had slit-shaped pores or the space between platelike particles, according to the classification of IUPAC (*34*).

The specific volumes of mesopores (2 nm ≤ pore diameter ≤ 50 nm) (V_m) and total pores smaller than 300 nm (V_t) of a sorbent are listed in Table 2; the total pore volume is only slightly larger than the mesopore volume. The pore volume of the raw BFS is very small since it is a fused material, but the treated HBFS and GBFS have appreciable pore volumes. The BFS/HL (10/90−90/10) sorbents also have much larger pore volumes than $Ca(OH)_2$ alone has. These results indicate that the new substances formed in the hydration process had created a highly porous sorbent structure. Among the sorbents, the HBFS/HL sorbent with a ratio of 50/50 has the largest mesopore and total pore volumes. On the whole, the BFS/HL ratio, slurrying temperature, and slurrying time affected the specific pore volume of sorbent in a manner similar to that they did on the specific surface area. In general, the specific pore volume increased as the specific surface area increased.

Reactivities of Sorbents. The sorbents were reacted with SO_2 at 60 °C, 70% RH, and 1000 ppm SO_2 for 1 h. The reaction time was long enough for a sorbent to reach the ultimate extent of reaction. The results expressed in terms of the utilization of Ca, X, and the SO_2 capture, SC, are summarized in Table 2. At least two repeated measurements were made for each kind of sorbent. The experimental error of Ca utilization was about ±0.02, and that of SO_2 capture was about ±0.02 g SO_2/g sorbent.

Effects of BFS/HL Weight Ratio and Slag Particle Size. Figure 4 presents the utilization of Ca and the SO_2 capture of sorbent versus the BFS weight fraction in the starting solid mixture for the HBFS/HL and GBFS/HL sorbents prepared

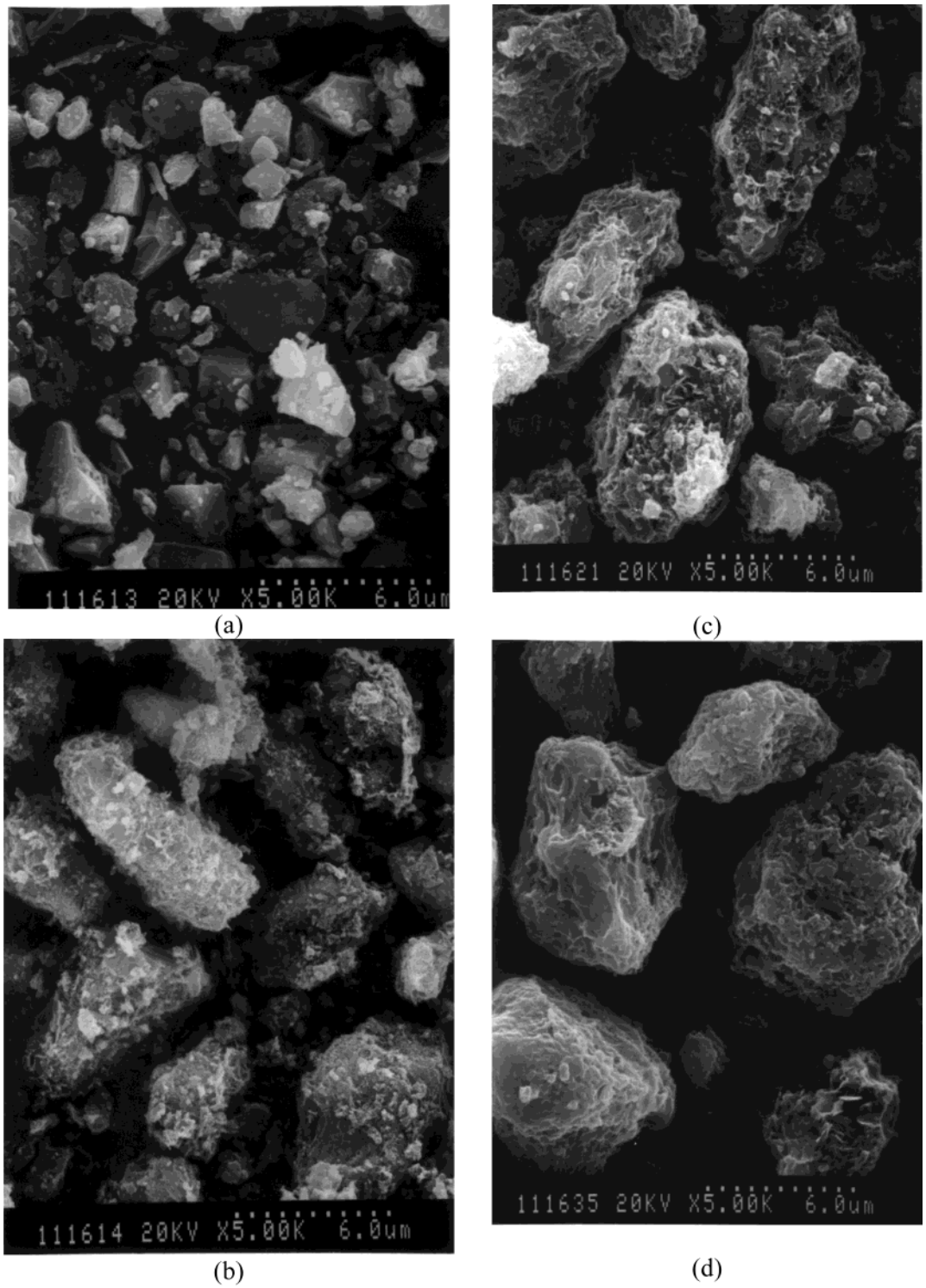

FIGURE 3. SEM micrographs of (a) raw HBFS; (b) treated HBFS; (c) HBFS/HL (30/70 wt ratio) sorbent; (d) HBFS/HL (30/70 wt ratio) sorbent reacted at 60 °C, 70% RH, and 1000 ppm SO_2 for 1 h. Slurrying conditions of samples of (b), (c), and (d): 65 °C, L/S = 10/1, and 16 h.

with different BFS/HL ratios. At each ratio, the HBFS/HL sorbent is more reactive than the GBFS/HL sorbent. The utilization of Ca and the SO_2 capture of sorbent vary significantly with the BFS/HL ratio, and both reach the maximum values when the ratio is 30/70. The maximum utilizations of Ca are 0.70 and 0.61 and the maximum SO_2 captures are 0.46 and 0.40 g SO_2/g sorbent for HBFS/HL and GBFS/HL sorbents, respectively. The best BFS/HL ratio was further determined experimentally to be in the range from 30/70 to 35/65.

As estimated from Figure 4, the utilization of Ca of sorbent would be higher than that of $Ca(OH)_2$ alone (0.24) if the ratio was smaller than 96/4 for the HBFS/HL sorbent or 94/6 for the GBFS/HL sorbent. Also, the SO_2 capture of sorbent would be higher than that of $Ca(OH)_2$ alone (0.20 g SO_2/g sorbent) if the weight ratio was smaller than 89/11 for the HBFS/HL sorbent or 72/28 for the GBFS/HL sorbent.

The raw HBFS and GBFS are nearly unreactive; their utilizations of Ca were only 0.03 and 0.02, respectively. But the treated ones (100/0) had utilizations of Ca of 0.11 and

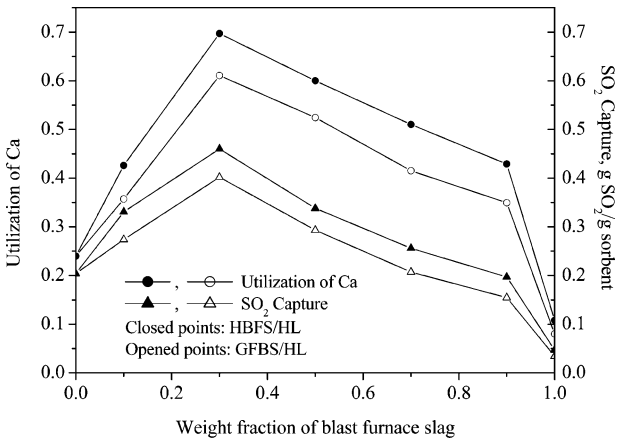

FIGURE 4. Effects of weight fraction and particle size of iron blast furnace slag on the utilization of Ca and the SO_2 capture for BFS/HL sorbents; slurrying conditions: 65 °C, L/S = 10/1, and 16 h; reaction conditions: 60 °C, 70% RH, and 1000 ppm SO_2 for 1 h.

0.08, respectively. This indicates that the hydration products of the slag are reactive toward SO_2.

From the results of sulfation tests and XRD analyses, one can conclude that the HL and hydration products in a BFS/HL sorbent are responsible for the sorbent reactivity. The sorbent reactivity is not only affected by their reactivities toward SO_2 but also by their particle characteristics. The formation of foil-like hydration products resulted in sorbents with much larger reactive surface areas and more porous structures than those of the raw $Ca(OH)_2$ and slag. Also, the HL particles in a BFS/HL sorbent were finer than the particles of the raw $Ca(OH)_2$ due to the dissolution and recrystallization processes. These facts may be the reason for the high reactivities of the BFS/HL sorbents.

However, the Ca contained in the sorbents was not fully utilized to capture SO_2; the highest utilization of Ca among the sorbents tested was 0.72, for which the sorbent was prepared with a HBFS/HL ratio of 30/70 and 32 h slurrying time. That $Ca(OH)_2$ and other reactive materials in the sorbents were not completely converted was also indicated by the XRD analyses of the reacted samples (Figure 2). The incomplete utilization of Ca of a sorbent is thought to result from the fact that the Ca contained in slag particles was not totally converted to reactive materials during the hydration process and that the sulfation product $CaSO_3 \cdot 0.5H_2O$ covered the surfaces of the HL and other reactive materials and stopped the reaction (*3*).

According to Lin et al. (*22*), under the same sorbent preparation and sulfation conditions as those of Figure 4, sorbents prepared from fly ash and hydrated lime also showed a maximum SO_2 capture at a ratio of 30/70. The SO_2 capture and the utilization of Ca for that sorbent were 0.38 g SO_2/g sorbent and 0.62, respectively. These values are smaller than the maximum values for the HBFS/HL sorbents but are close to those for the GBFS/HL sorbents. This comparison indicates that BFS can be better than fly ash for preparing reactive SO_2 sorbents.

Effects of Slurrying Conditions. As seen from Table 2, the utilization of Ca and the SO_2 capture for an HBFS/HL (30/70) sorbent increase in general with increasing slurrying time. However, the utilization of Ca has already reached 0.60 for a slurrying time of 0.42 h, and the increment is not marked thereafter, only 0.05 in the period of 8−32 h. This result is due to that in the beginning of hydration, the compounds in the surface layers of slag particles started to ionize, and the silicate and aluminate ions then combined with the Ca ions, originating from the slag or the $Ca(OH)_2$ solution, to form products of low solubility which precipitated on or around the surfaces of slag particles; thus the hydration rate of slag was slowed by the formation of product layer on the particle surface, and accordingly the amounts of hydration products increased only slowly afterward. This explanation is in agreement with the results of sorbent characterization.

TABLE 3. Effect of Drying Conditions on the Reactivities of HBFS/HL Sorbent[a]

drying conditions				
temp (°C)	press (atm)	time (h)	X	SC (g SO_2 /g sorbent)
35	0	24	0.66	0.43
105	0	2	0.65	0.43
105	1	8	0.68	0.44
105	1	16	0.67	0.44
105	1	168	0.70	0.45

[a] Slurrying conditions: 65 °C, 30/70 wt ratio, L/S = 10/1, and 16 h; sulfation conditions: 60 °C, 70% RH, 1000 ppm SO_2, and 1 h.

From Table 2, one can see that both the utilization of Ca and the SO_2 capture for an HBFS/HL (30/70) sorbent increase markedly with increasing slurrying temperature until 65 °C and level off thereafter. The utilization of Ca rises from 0.39 (25 °C) to 0.70 (65 °C). The effect of slurrying temperature may indicate that at low temperatures the hydration rate of slag was controlled by surface reaction and at high temperatures by product layer diffusion.

As shown in Table 2, the utilizations of Ca and the SO_2 captures for HBFS/HL (30/70) sorbents prepared with L/S ratios of 10/1 to 20/1 are almost the same and are higher than those for the one prepared with 5/1 ratio; however, the differences are not large, about 0.10 in the utilization of Ca. As discussed above, the content of reactive hydration products in a sorbent was controlled by the hydration rate of slag. At the slurrying conditions of these HBFS/HL (30/70) sorbents, the hydration rate of slag might depend only on the total slag surface area in the early stage of slurrying and on the pore structure of the product layer in the latter stage, thus the effect of L/S ratio would be absent. However, if the L/S ratio was too small, the hydration products formed would have a greater tendency to cover the slag particles, thus the hydration rate would slow earlier and the amounts of reactive materials formed would be less than those formed at high L/S ratios after the same slurrying time.

Effect of Drying Conditions. The reactivities of sorbents which were prepared under the same slurrying conditions but dried under different drying conditions are compared in Table 3. The reactivities of samples obtained by vacuum-drying at 35 °C for 24 h and 105 °C for 2 h are the same. The reactivities of the samples obtained by drying at ambient pressure and 105 °C for 8−168 h are also about the same. The maximum difference between the data in Table 3 is comparable to the range of experimental error (±0.02 in Ca utilization). These results indicate that the pressure, temperature, and time used to dry the slurry to the dry solid state had no significant effect on the reactivity of the sorbent obtained.

Effects of Structural Properties. From Table 2, one can see that the utilization of Ca or the SO_2 capture of sorbent increases with increasing S_{g0} for sorbents prepared with a BFS/HL ratio of 30/70. But for sorbents prepared with various BFS/HL ratios, although the utilization of Ca or the SO_2 capture increases in general with increasing S_{g0}, the scattering of the data is large, indicating that S_{g0} is not the only factor affecting the sorbent reactivity. After an extensive search, it was found that the utilization of Ca was best correlated with S_{g0}/M. As shown in Figure 5, when the utilization of Ca is plotted against S_{g0}/M, the data are less scattered and are almost linearly correlated. By least-squares fitting to the data

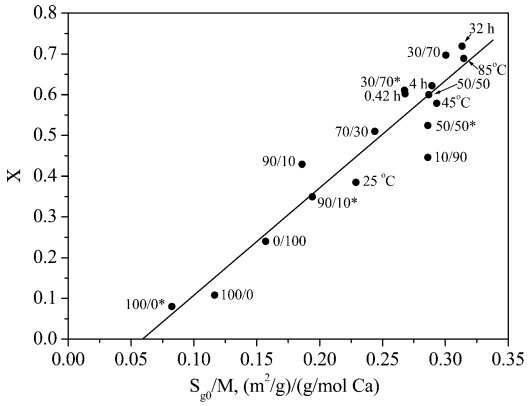

FIGURE 5. Relationship between the utilization of Ca and S_{g0}/M for BFS/HL sorbents. Sorbent preparation and sulfation conditions are listed in Table 2. Labels indicate the major preparation condition of the sorbent.

in Figure 5, the correlation obtained is

$$X = -0.16 + 2.6S_{g0}/M \quad (2)$$

for which the correlation coefficient is 0.95 and the standard deviation of X is 0.06. Since M^{-1} is the molar content of Ca in an unreacted sorbent, it is proportional to the initial weight fraction of Ca in that sorbent. Thus, eq 2 indicates that the ultimate utilization of Ca of a sorbent is proportional to its S_{g0} as well as its initial Ca weight fraction. This implies that the reaction took place at the surface where Ca atoms locate. From eqs 1 and 2, one can get the correlation among the SO_2 capture, S_{g0}, and M:

$$SC = -9.9/M + 170S_{g0}/M^2 \quad (3)$$

Furthermore, as discussed before, the specific mesopore volume increases in general with increasing S_{g0}, thus, the utilization of Ca also increases in general with increasing V_m/M; however, it was found that the correlation with V_m/M is not as good as that with S_{g0}/M.

Nomenclature

BFS	iron blast furnace slag
d_P	volume mean particle diameter, μm
FGD	flue gas desulfurization
GBFS	general fineness iron blast furnace slag
HBFS	high fineness iron blast furnace slag
HL	hydrated lime
L/S	water/solid weight ratio
M	initial sorbent weight per mole of Ca, g sorbent/mol Ca
M_{SO_2}	molecular weight of SO_2, g/mol
RH	relative humidity, %
SC	SO_2 capture, kg SO_2/kg sorbent
S_{g0}	initial specific surface area, m^2/g
V_m	initial specific mesopore volume, cm^3/g
V_t	initial specific total pore volume, cm^3/g
X	the utilization of Ca, -

Acknowledgments

This research was supported by the National Science Council of the Republic of China (Taiwan).

Literature Cited

(1) Miller, M. J. *Environ. Prog.* **1986**, *3*, 171−177.
(2) Srivastava, R. K.; Jozewicz, W. *J. Air Waste Manage. Assoc.* **2001**, *51*, 1676−1688.
(3) Ho, C. S.; Shih, S. M.; Liu, C. F.; Chu, H. M.; Lee, C. D. *Ind. Eng. Chem. Res.* **2002**, *41*, 3357−3364.
(4) Jozewicz, W.; Rochelle, G. T. *Environ. Prog.* **1986**, *5*, 219−224.
(5) Peterson, J. R.; Rochelle, G. T. *Environ. Sci. Technol.* **1988**, *22*, 1299−1304.
(6) Peterson, J. R.; Rochelle, G. T. *Proceedings of 1990 SO_2 Control Symposium*, New Orleans, LA, 1990; pp 3−24.
(7) Peterson, J. R. Ph.D. Dissertation, University of Texas in Austin, 1990.
(8) Martinez, J. C.; Izquierdo, J. F.; Cunill, F.; Tejero, J.; Querol, J. *Ind. Eng. Chem. Res.* **1991**, *30*, 2143−2147.
(9) Diffenbach, P.; Hilterman, M.; Frommell, E.; Boother, H.; Hedges, S. *Thermochim. Acta* **1991**, *189*, 1−24.
(10) Ho, C. S.; Shih, S. M. *Ind. Eng. Chem. Res.* **1992**, *31*, 1130−1135.
(11) Ho, C. S.; Shih, S. M. *Can. J. Chem. Eng.* **1993**, *71*, 934−939.
(12) Kind, K. K.; Wasserman, P. D.; Rochelle, G. T. *Environ. Sci. Technol.* **1994**, *28*, 277−283.
(13) Kind, K. K.; Rochelle, G. T. *J. Air Waste Manage. Assoc.* **1994**, *44*, 869−876.
(14) Sanders, J. R.; Keener, C. T.; Wang, J. *Ind. Eng. Chem. Res.* **1995**, *34*, 302−307.
(15) Tsuchiai, H.; Ishizuka, T.; Ueno, T.; Hattori, H.; Kita, H. *Ind. Eng. Chem. Res.* **1995**, *34*, 1404−1411.
(16) Al-Shawabkeh, A.; Matsuda, H.; Hasatani, M. *J. Chem. Eng. Jpn.* **1995**, *28*, 53−58.
(17) Garea, A.; Viguri, J. R.; Irabien, J. A. *Chem. Eng. Sci.* **1997**, *52*, 715−732.
(18) Fernández, J.; Renedo, M. J.; Garea, A,; Viguri, J. R.; Irabien, J. A. *Powder Technol.* **1997**, *94*, 133−139.
(19) Renedo, M. J.; Fernández, J.; Garea, A.; Ayerbe, A.; Irabien, J. A. *Ind. Eng. Chem. Res.* **1999**, *38*, 1384−1390.
(20) Ishizuka, T.; Tsuchiai, H.; Murayama, T.; Tanaka, T.; Hattori, H. *Ind. Eng. Chem. Res.* **2000**, *39*, 1390−1396.
(21) Liu, C. F.; M. Shih,S.; Lin, R. B. *Chem. Eng. Sci.* **2002**, *57*, 93−104.
(22) Lin, R. B.; Shih, S. M.; Liu, C. F. *Ind. Eng. Chem. Res.* **2003**, *42*, 1350−1356.
(23) Jozewicz, W.; Jorgensen, C.; Chang, J. C. S.; Sedman, C. B.; Brna, T. G. *JAPCA* **1988**, *38*, 796−805.
(24) Jozewicz, W.; Jorgensen, C.; Chang, J. C. S.; Sedman, C. B.; Brna, T. G. *JAPCA* **1988**, *38*, 1027−1034.
(25) Jung, G. H.; Kim, H.; Kim, S. G. *Ind. Eng. Chem. Res.* **2000**, *39*, 1264−1270.
(26) Jung, G. H.; Kim, H.; Kim, S. G. *Ind. Eng. Chem. Res.* **2000**, *39*, 5012−5016.
(27) Chiu, C. S. M.S. Thesis, National Taiwan University, Taipei, Taiwan, 1989.
(28) Chiang, S. T. M.S. Thesis, National Taiwan University, Taipei, Taiwan, 1994.
(29) Kind, K. K. Ph.D. Dissertation, University of Texas in Austin, 1994.
(30) Lin, R. B. M.S. Thesis, National Taiwan University, Taipei, Taiwan, 1998.
(31) Liu, C. F. M.S. Thesis, National Taiwan University, Taipei, Taiwan, 1999.
(32) Brodnax, L. F.; Rochelle, G. T. *J. Air Waste Manage. Assoc.* **2000**, *50*, 1655−1662.
(33) Taylor, H. F. W. *The Chemistry of Cement*; Academic Press: London, 1964; Vol. I and II.
(34) IUPAC. *Pure Appl. Chem.* **1985**, *57*, 603−619.

Received for review February 3, 2003. Revised manuscript received August 21, 2003. Accepted June 2, 2004.

ES030347C